IEEE INSTRUMENTATION & MEASUREMENT SOCIETY

Received 5 June 2022; revised 20 July 2022; accepted 1 August 2022. Date of publication 15 August 2022; date of current version 6 September 2022.
The review of this paper was arranged by Associate Editor Roberto Ferrero.

Digital Object Identifier 10.1109/OJIM.2022.3198470

Distributed State Estimation for Multi-Feeder Distribution Grids

MARCO PAU [1] (Member, IEEE), FERDINANDA PONCI [2] (Senior Member, IEEE), ANTONELLO MONTI [2] (Senior Member, IEEE), CARLO MUSCAS [3] (Senior Member, IEEE), AND PAOLO ATTILIO PEGORARO [3] (Senior Member, IEEE)

[1]Department of Grid Planning and Operation, Fraunhofer Institute for Energy Economics and Energy System Technology, 34119 Kassel, Germany

[2]Institute for Automation of Complex Power Systems, RWTH Aachen University, 52062 Aachen, Germany

[3]Department of Electrical and Electronic Engineering, University of Cagliari, 09123 Cagliari, Italy

CORRESPONDING AUTHOR: M. PAU (e-mail: marco.pau@iee.fraunhofer.de)

The work of Paolo Attilio Pegoraro was supported in part by the Fondazione di Sardegna for the Research Project "IQSS, Information Quality Aware and Secure Sensor Networks for Smart Cities," year 2020.

ABSTRACT The real-time monitoring of electric distribution grids via state estimation is a fundamental requirement to deploy smart automation and control in the distribution system. Due to the large size of distribution networks and the poor coverage of measurement instrumentation on the field, designing fast state estimation algorithms and achieving accurate results are two major challenges associated to distribution system state estimation. In this paper, an efficient and accurate solution for performing state estimation in multi-feeder radial distribution grids is presented. The proposed algorithm is based on a two-step approach. In the first step, state estimation is performed in parallel on the different feeders suitably processing the available measurements and pseudo-measurements and taking into account their uncertainty characteristics. In the second step, the results on each feeder are post-processed to refine the estimations and to improve the accuracy performance. To this purpose, the second step considers how measurement uncertainties propagate towards the final estimates and how measurements shared among the feeders could adversely affect the final estimation. Performed tests show that the conceived design leads to accuracy performance very close to those achievable by running state estimation on the full grid. At the same time, the parallelization of the estimation process on the different feeders allows decentralizing the state estimation problem, with the associated benefits in terms of computation time and distribution of the communication and storage requirements.

INDEX TERMS Distribution grid, distribution management system, distribution system state estimation, measurement uncertainty, multi-area state estimation, smart grid.

I. INTRODUCTION

DISTRIBUTION System State Estimation (DSSE) is a key component of the Distribution Management System (DMS) envisaged for the management of future distribution networks [1], [2]. The role of the DSSE is to process the measurements coming from the instrumentation on the field for providing the real-time operating conditions of the grid. This output gives situational awareness to Distribution System Operators (DSOs) and enables advanced management functionalities, such as volt/var control, network topology reconfiguration, distributed energy resources control, and others [3]. Due to the very large size of distribution networks, a critical aspect for DSSE is to find solutions for reducing and/or distributing the computational burden. A possible idea in this direction is the adoption of Multi-Area State Estimation (MASE) techniques. MASE approaches have been largely investigated in the context of transmission systems, mainly with the goal of coordinating different

local estimations to achieve the monitoring of wide area systems [4], [5], [6], [7], [8]. Several solutions have been proposed, which can be classified depending on the level of overlapping among areas (no, minimum or extended overlapping), underlying architecture (centralized or decentralized), and type of coordination process (at SE or iteration level) [9].

While the methodologies proposed for transmission represent a good benchmark for the MASE design, their direct migration to the distribution network is not possible due to the specific characteristics of the distribution system. A major obstacle is the different level of measurement availability. In fact, transmission grids usually rely on a largely redundant measurement infrastructure, whereas distribution systems typically have only few measurement devices [10]. As a consequence, the partition of the network in multiple areas can be constrained by the meter location and approaches based on the use of redundant measurements in the boundary zones are not applicable. The poor coverage of measurements also poses specific requirements for the design of the MASE approach. In particular, since highly uncertain pseudo-measurements (namely forecasts of power generation or consumption at the nodes) are commonly used to reach the observability at distribution level, the design of the MASE scheme has to duly consider the DSSE accuracy performance and should possibly minimize the degradation of the estimation results with respect to the Integrated State Estimation (ISE) applied to the full grid.

In the literature, only few proposals can be found for MASE approaches specifically conceived for the distribution grid scenario. In [11], [12], [13], hierarchical schemes have been proposed to decouple the estimation process according to the voltage level of the grid. Such approaches allow the integration of estimation results in the upper level of the hierarchy, but are not conceived to handle the horizontal partition of the network (multiple areas belonging to the same voltage level). In [14], a zonal approach is used to split the medium voltage (MV) network in several areas, which are processed independently using in series or in parallel execution. However, the harmonization of the local results is not addressed in details, and this could lead to an important degradation of the accuracy performance. In [15], an evolutionary algorithm is used to run local DSSE processes in different areas and the coordination is obtained through the exchange of data at each iteration of the algorithm. This minimizes the accuracy degradation with respect to ISE, but brings heavy computation expenses and hard communication requirements. The approach in [16] proposes a partition in zones with overlapping buses. The harmonization among different areas is achieved through multiple zonal interactions occurring after each local DSSE execution. This allows refining the estimation results, but several zonal interactions are needed, thus limiting the potential to reduce the overall computation times.

The Authors of this work also proposed possible MASE solutions for distribution grids in previous papers. In [17], a two-step approach was presented, based on local estimations at the first step and an harmonization procedure at the second step. In particular, [17] highlighted the impact of correlations brought by measurements shared among multiple areas during the harmonization process and proposed a solution to cope with this issue and improve the estimation accuracy. In [18], a simpler and improved version of the MASE scheme has been presented, which uses a modified Weighted Least Squares (WLS) approach for the second step harmonization.

In the paper presented here, a two-step MASE approach specific for radially operated distribution grids with multiple feeders is presented. With respect to previous works, the goal is to propose a solution tailored for this common distribution grid configuration and to refine the estimation process carefully considering the impact of measurement configuration on both the voltage and current estimates. While the proposed technique exploits some of the analytical findings presented in [18] for the refinement of the voltage at the second step, a new solution is proposed to improve the second step estimation of the branch currents. This allows reaching accuracy performance very close to the ISE both for the bus voltage profile and for the current and power flow estimation, while guaranteeing the advantages associated to the decentralization of the DSSE on each feeder. Moreover, this work proposes a method to integrate the bad data detection and identification functionalities in the MASE scheme, thus offering robustness to measurements with anomalous errors.

The rest of the paper is structured as follows. Section II presents the two-step approach followed for the MASE implementation and shows the architecture design applicable to the MASE scheme. In Section III, the details on the integration and bad data detection process performed at the second step of the MASE algorithm are presented. Section IV provides the details of the set-up used for the tests. The performance achievable with the conceived solution is then discussed in Section V, by presenting the results of ad hoc simulations in several test cases. Finally, Section VI provides the final remarks and concludes the paper.

II. MULTI-FEEDER STATE ESTIMATION

Distribution grids are often operated with a radial topology, since this configuration facilitates the coordination of automation and protections. For this reason, several works propose solutions tailored to the radial topology of distribution systems, e.g., for power flow computation and network operation [19], [20], [21]. Radial distribution grids are often composed of multiple feeders, which constitute the backbone of the network and provide the connection for the laterals supplying end-users and, in case of MV grids, secondary substations [22]. Examples of real distribution grids characterized by multi-feeder radial topology, or having meshed topology but being operated as an open ring (by means of tie-lines), can be found, for instance, in [23], [24], [25], [26]. The MASE solution proposed in this paper is tailored to this topology and allows decoupling the monitoring of each feeder, while achieving performance very close to those of the DSSE on the full grid. In the following, the benefits

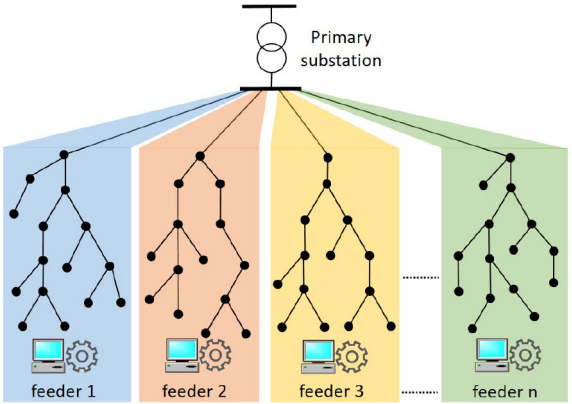

FIGURE 1. Multi-feeder decentralized DSSE architecture.

associated to the envisioned decentralized architecture and the two-step algorithm at the basis of the proposed MASE design are presented.

A. MASE ARCHITECTURE

The aim of the MASE design presented in this paper is to decouple the DSSE execution among the different feeders, so that each feeder estimation can be carried out independently and in parallel. The conceived MASE architecture can be thus decentralized, with each feeder possibly having a control unit responsible for the local DSSE execution and for providing the monitoring results necessary to the DSO. Fig. 1 shows an example of distribution grid, operated radially, with its partition in multiple feeders according to the lines departing from the main substation. The main benefits associated to a decentralized architecture are:

1) the DSSE computation burden is distributed among the different feeder control units, which can work in parallel and on smaller size problems;
2) data communication is also distributed: each control unit collects only the measurements coming from the instrumentation connected to the feeder it supervises;
3) storage is distributed: grid data and other information needed for the DSSE are stored in the different control units according to the feeder they belong to;
4) robustness: each feeder control unit works independently and provides meaningful estimation for its sub-network regardless of possible issues on the other control units;
5) redundancy: each feeder control unit can be configured to provide back-up computational resources in case one of the other control units has technical issues.

As described in the next section, the proposed MASE solution is based on a two-step algorithm. In the second step, some of the results obtained by the different feeder control units are collected and post-processed in order to refine the estimation results and to improve in this way the accuracy performance. For the second step execution, each feeder control unit receives the needed data from the other control units and performs the harmonization process locally.

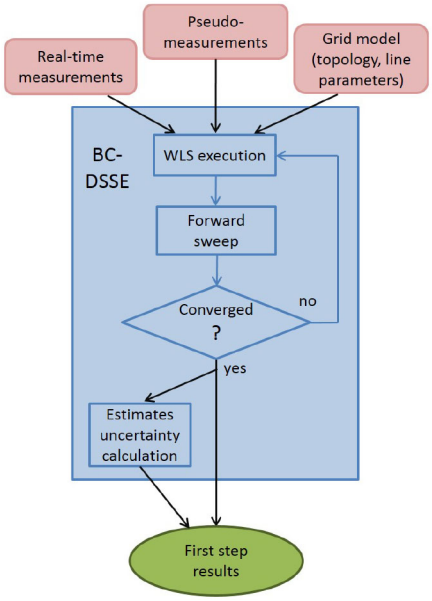

FIGURE 2. Flowchart of the MASE first step.

As a consequence, both the steps of the MASE are performed locally, allowing a fully decentralized architecture.

B. MASE ALGORITHM

The proposed MASE algorithm is based on a two-step procedure. In the following, the details of each step are given.

1) FIRST STEP ALGORITHM

At the first step of the MASE, each control unit performs the DSSE for the portion of grid associated with the monitored feeder (see Fig. 1). In the considered scenario, the main substation bus is shared among all the feeders and therefore this node is included in the grid model of each DSSE. To solve the DSSE, the rectangular branch-current formulation proposed in [27] is used in this paper. However, it is worth noting that any other Weighted Least Squares (WLS) formulation, also based on different state variables, can be applied to perform the first-step DSSE.

Fig. 2 gives an overview of the algorithm used at this stage. The algorithm takes as input all the real-time measurements available in the monitored feeder, together with the pseudo-measurements needed to achieve the grid observability and the model of the corresponding portion of grid. It is worth noting that measurements are often placed at the main substation. Among them, the voltage measurement at the substation bus and the current or power measurement at the departure of the feeder (when available) are included in the set of input measurements. On the contrary, the measurement of the total power or current through the substation transformer is not taken in input at this stage since it does not represent an equivalent injection for any of the feeders (it would be the sum of the injections in all the feeders). Given these inputs, the DSSE computes the estimates of the

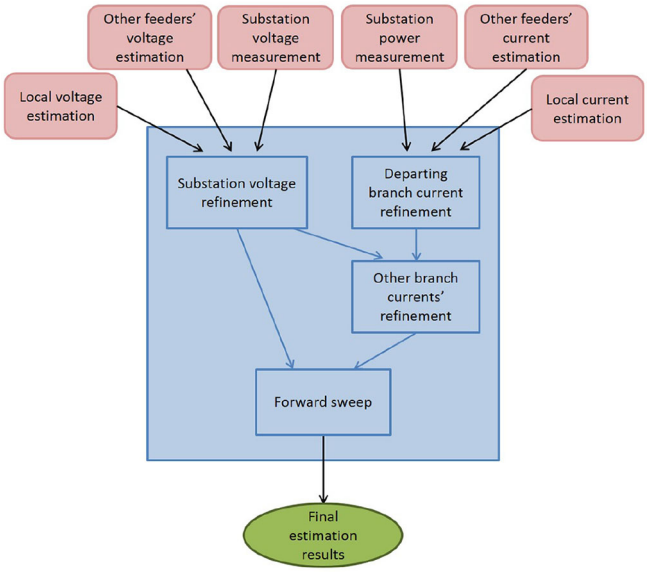

FIGURE 3. Flowchart of the MASE second step.

branch currents and, via a forward sweep, the node voltages (see [27] for details). After the convergence of the DSSE, the uncertainty of the estimated quantities is also extracted. The inverse of the so-called Gain matrix is used to calculate the covariance matrix of the quantities directly estimated by the estimator (branch currents with the formulation used here) and the law of propagation of uncertainty is used to derive the uncertainty of the other quantities (node voltages and current injections for the case at hand).

2) SECOND STEP ALGORITHM

The goal of the MASE second step is to refine the first-step estimates by using the estimation results obtained in the other feeders. Fig. 3 shows the flowchart of the second-step algorithm. At the beginning, each feeder control unit receives the voltage estimated at the substation bus and the current estimated in the departing branch of the feeder from all the other control units. These estimates are then post-processed together with the same results obtained locally and with the measurements of voltage and total power (or current) at the substation. This allows refining the estimation of the substation voltage and of the current at the departure of each feeder. These new values are then used to update also the other branch currents and voltages of each feeder, giving in this way the final estimation for the whole monitored area. The mathematical formulations used to perform the tasks described here are presented more in detail in the next Section III.

In addition to the benefits described in Section II-A, the conceived MASE design brings the following features:

1) communication requirements: data exchange occurs only once (for each estimation) and very low data transmission is needed to enable the second-step harmonization.
2) robustness: in case of communication failure for one of the control units, the other areas can still take benefit from the results provided by the remaining feeders; for the faulty unit, the first-step estimation can be still used as result (even if this has lower accuracy).
3) simplicity: the second-step process is based on a very simple WLS procedure, which can be easily implemented in any programming language and platform.

III. MULTI-FEEDER HARMONIZATION PROCESS

The harmonization process implemented at the second step refines the first-step estimates by integrating the estimation results provided by the other feeder control units. Two different WLS-based procedures are used for the refinement of voltage and branch current estimations, respectively. Next sections provide the mathematical details of the second-step algorithms.

A. VOLTAGE REFINEMENT

The procedure followed to refine the voltage profile is derived from the analytical findings and the WLS formulation presented in [18]. Mapping that procedure to the scenario presented in this paper, first of all, a WLS algorithm is applied to update the estimation of the voltage at the substation bus. The algorithm adopted to this purpose uses the substation bus voltage V_s as only state variable and the vector of the substation voltage estimates $\hat{\mathbf{v}}$, computed by the different feeder units at the first step, as input measurements. The weights of the first-step estimates needed for the WLS model are calculated as the inverse of their estimation variance (which is obtained at the end of the first-step process) and used to build the corresponding diagonal weighting matrix $\mathbf{W}_{\hat{v}}$.

As proved in [18], in addition to the first-step estimates, the voltage measurement at the substation node $V_{s,\text{meas}}$ has also to be used in input to the WLS to maximize the estimation accuracy. In fact, since this voltage measurement is used in all the first-step feeder estimations, it is necessary to take it into account to avoid a too large influence of such a measurement into the final result. To this purpose, this measurement is integrated into the WLS using a negative weight equal to $-(n-1)\cdot W_{V_{s,\text{meas}}}$, where n is the number of feeders in the grid and $W_{V_{s,\text{meas}}}$ is the weight calculated as the inverse of the measurement variance.

Summarizing, the following WLS calculation is implemented to update the substation bus voltage estimation (superscript ^{T} indicates the transpose operator):

$$\mathbf{H}_V^T\mathbf{W}_V\mathbf{H}_V\cdot V_s = \mathbf{H}_V^T\mathbf{W}_V\cdot\mathbf{z}_V \tag{1}$$

where $\mathbf{H}_V$ is the Jacobian, which in this case is a $n+1$ size vector of ones, $\mathbf{W}_V$ is the overall weighting matrix built as

$$\mathbf{W}_V = \begin{bmatrix} \mathbf{W}_{\hat{v}} & 0 \\ 0 & -(n-1)W_{V_{s,\text{meas}}} \end{bmatrix} \tag{2}$$

and $\mathbf{z}_V$ is the input vector defined as

$$\mathbf{z}_V = \left[\hat{\mathbf{v}}^T, V_{s,\text{meas}}\right]^T \tag{3}$$

It is worth noting that, since the designed WLS formulation is based on a linear measurement model, the solution of (1) is direct (it does not require an iterative process). Moreover, the Gain matrix $\mathbf{G}_V = \mathbf{H}_V^T \mathbf{W}_V \mathbf{H}_V$ on the left side of (1) is a scalar and its inversion is, therefore, straightforward. As a result, the overall procedure to update the substation bus voltage corresponds to a weighted average of the input quantities and is very simple and fast. It should be noted that all the feeder units use exactly the same set of inputs for the WLS algorithm (all the first-step estimates and the direct measurement of the substation voltage). Thus, they will achieve the same estimation result for the substation voltage at the end of the second step, making their local estimations fully consistent. Finally, no grid data exchange is necessary between units, thus allowing each unit to see the rest of the network as a black-box represented by its starting voltage.

It is important to underline that, when absolute phase angles of voltages can be also estimated (i.e., in the presence of synchronized phasor measurements), a similar second step can be applied to the substation bus voltage phase angle to refine first-step estimates and compute the estimated phasor. In the presence of traditional measurements instead (as in the following), the substation phase angle is conventionally assumed as zero. Once the substation bus voltage has been refined, the rest of the node voltages in the feeder can be updated via a forward sweep procedure, computing the voltage drops in the lines. To this purpose, the updated values of the branch currents obtained in the second step (whose calculation is described in the following section) need to be used.

B. BRANCH CURRENT REFINEMENT

Similar to the voltage estimation, a simplified WLS procedure is adopted for the refinement of the branch currents. The aim is to integrate, when available, the measurement of power at the substation transformer to refine the estimation of the currents of each feeder. To this purpose, the currents at the departing branch of each feeder are used as state variables in this WLS. The corresponding first-step estimates are used as inputs to the WLS model, together with the measurement of the total power at the substation transformer. This power measurement is converted into an equivalent current by using the second-step substation bus voltage estimation as follows:

$$I_s^{re} + jI_s^{im} = \frac{P_s \hat{V}_s^{re} + Q_s \hat{V}_s^{im}}{\hat{V}_s^2} + j\frac{P_s \hat{V}_s^{im} - Q_s \hat{V}_s^{re}}{\hat{V}_s^2} \tag{4}$$

where I_s^{re} and I_s^{im} are the real and imaginary component of the current, P_s and Q_s are the measured active and reactive power, and $\hat{V}_s$, $\hat{V}_s^{re}$ and $\hat{V}_s^{im}$ are the magnitude, real and imaginary part of the estimated substation bus voltage.

Given these state variables and inputs, the WLS model is

$$\mathbf{H}_I^T \mathbf{W}_I \mathbf{H}_I \cdot \mathbf{x} = \mathbf{H}_I^T \mathbf{W}_I \cdot \mathbf{z}_I \tag{5}$$

The state vector $\mathbf{x}$ is

$$\mathbf{x} = \left[I_{11}^{re}, I_{21}^{re}, \ldots, I_{n1}^{re}, I_{11}^{im}, I_{21}^{im}, \ldots, I_{n1}^{im} \right]^T \tag{6}$$

with I_{i1}^{re} and I_{i1}^{im} being the real and imaginary part of the current at the departing branch (branch 1) of the i-th feeder.

The input vector $\mathbf{z}_I$ is

$$\mathbf{z}_I = \left[\hat{\mathbf{i}}^{re^T}, \hat{\mathbf{i}}^{im^T}, I_s^{re}, I_s^{im} \right]^T \tag{7}$$

where $\hat{\mathbf{i}}^{re}$ and $\hat{\mathbf{i}}^{im}$ are the vectors containing the first-step estimates of the real and imaginary part of the currents at the departing branch of each feeder (i.e., of the state variables).

Finally, $\mathbf{H}_I$ and $\mathbf{W}_I$ are the Jacobian and the weighting matrix. The Jacobian matrix has only a non-zero element (equal to 1) in each row associated to derivatives with respect to a first-step estimate, whereas it has all the elements equal to 1 for the row with the derivatives of the total real (or imaginary) current with respect to the real (or imaginary) branch current variables. The weighting matrix is instead chosen as a diagonal matrix with the weights derived as usual from the variances obtained during the first-step estimation for each of the input estimated currents and from instrument specifications for total current measurements.

As a result of this WLS procedure, a new vector $\hat{\mathbf{x}}$ of currents at the departing branch of each feeder is obtained. These results will differ with respect to the first step estimates according to the following:

$$\delta I_{i1}^{re} = \hat{I}_{i1,\text{new}}^{re} - \hat{I}_{i1,1^{\text{st}}}^{re} \tag{8}$$

$$\delta I_{i1}^{im} = \hat{I}_{i1,\text{new}}^{im} - \hat{I}_{i1,1^{\text{st}}}^{im} \tag{9}$$

where $\hat{I}_{i1,\text{new}}^{c}$ and $\hat{I}_{i1,1^{\text{st}}}^{c}$ (the superscript c can be either re or im) are the new results obtained through the described WLS procedure and the first step estimate, respectively, at the departing branch of the i-th feeder.

For each feeder i, an approximate but very fast refinement of all the branch currents is obtained considering the superimposition of the effects brought by two contributions: the first one is the current refinement obtained in (8) and (9) due to the integration of the overall power at the substation, while the second one is associated to the substation voltage refinement. Similar to eqs. (8) and (9), the refinement of the substation voltage described in Section III-A can be expressed as

$$\delta V_{si} = \hat{V}_{s,2^{\text{nd}}} - \hat{V}_{si,1^{\text{st}}} \tag{10}$$

where subscript i reminds that a different refinement can be achieved in each feeder starting from a different estimate of the bus voltage, while subscripts $_{1^{\text{st}}}$ and $_{2^{\text{nd}}}$ highlight the step producing the corresponding estimate.

For each branch k of the considered feeder i, the effect brought by the refinement of the generic variable Y (with $Y \in \{I_{i1}^{re}, I_{i1}^{im}, V_{si}\}$) on the associated current (both for the real and imaginary part) is considered by means of a sensitivity

factor computed as follows:

$$\delta I_{ik}^{c}(Y) = \frac{cov\left(\hat{I}_{ik,1^{st}}, \hat{Y}_{1^{st}}\right)}{var\left(\hat{Y}_{1^{st}}\right)} \cdot \delta Y \tag{11}$$

where $c \in \{re, im\}$, $cov(a, b)$ represents the covariance between the variables a and b and $var(b)$ indicates the variance of b. $\hat{Y}_{1^{st}}$ indicates the estimate of the quantity Y after the first step and δY is the variation in the same quantity due to the refinement. The sensitivity factor is thus resulting from the first step estimation.

Considering the three contributions in (8), (9) and (10) as decorrelated and thus applying the superimposition of the effects, the overall changes to be applied to the first step estimates of each branch current (i.e., to its real and imaginary parts) become:

$$\Delta I_{ik}^{re} = \sum_{Y \in \{I_{i1}^{re}, I_{i1}^{im}, V_{si}\}} \delta I_{ik}^{re}(Y) = \frac{cov\left(\hat{I}_{ik,1^{st}}^{re}, \hat{I}_{i1,1^{st}}^{re}\right)}{var\left(\hat{I}_{i1,1^{st}}^{re}\right)} \cdot \delta I_{i1}^{re} + \frac{cov\left(\hat{I}_{ik,1^{st}}^{re}, \hat{I}_{i1,1^{st}}^{im}\right)}{var\left(\hat{I}_{i1,1^{st}}^{im}\right)} \cdot \delta I_{i1}^{im} + \frac{cov\left(\hat{I}_{ik,1^{st}}^{re}, \hat{V}_{s,1^{st}}\right)}{var\left(\hat{V}_{si,1^{st}}\right)} \cdot \delta V_{si} \tag{12}$$

$$\Delta I_{ik}^{im} = \sum_{Y \in \{I_{i1}^{im}, I_{i1}^{im}, V_{si}\}} \delta I_{ik}^{im}(Y) = \frac{cov\left(\hat{I}_{ik,1^{st}}^{im}, \hat{I}_{i1,1^{st}}^{re}\right)}{var\left(\hat{I}_{i1,1^{st}}^{re}\right)} \cdot \delta I_{i1}^{re} + \frac{cov\left(\hat{I}_{ik,1^{st}}^{im}, \hat{I}_{i1,1^{st}}^{im}\right)}{var\left(\hat{I}_{i1,1^{st}}^{im}\right)} \cdot \delta I_{i1}^{im} + \frac{cov\left(\hat{I}_{ik,1^{st}}^{im}, \hat{V}_{si,1^{st}}\right)}{var\left(\hat{V}_{si,1^{st}}\right)} \cdot \delta V_{si} \tag{13}$$

Using the branch current formulation proposed in [27], the variance and covariance terms required to apply (12) and (13) are automatically obtained through the inversion of the Gain matrix of the first step WLS estimation. If a WLS formulation based on different state variables is used, the needed covariance and variance components should be computed by applying the uncertainty propagation law. It is worth noting that, in this process, the weights associated with the accuracies of the voltage and current estimates are directly reflected in the computation of the new estimates and thus in the differences computed in (8), (9) and (10).

Given the updating values of the real and imaginary branch currents as expressed in (12) and (13), the final (second step) estimations for the branch currents of each feeder i thus become (for the generic branch k):

$$\hat{I}_{ik,2^{nd}}^{re} = \hat{I}_{ik,1^{st}}^{re} + \Delta I_{ik}^{re} \tag{14}$$

$$\hat{I}_{ik,2^{nd}}^{im} = \hat{I}_{ik,1^{st}}^{im} + \Delta I_{ik}^{im} \tag{15}$$

C. BAD DATA HANDLING

Both steps of the proposed MASE are equipped with bad data processing routines based on the largest normalized residuals [28]. To this aim, the normalized residual r_m^N for the m-th measurement in the input vector $\mathbf{z}$ is computed as:

$$r_m^N = \frac{z_m - h_m(\mathbf{x})}{\mathbf{\Omega}_{mm}} \tag{16}$$

where $h_m(\mathbf{x})$ is the measurement function linked to considered measurement m and $\mathbf{\Omega}_{mm}$ is the m-th element of the diagonal of the residual covariance matrix, which is calculated as:

$$\mathbf{\Omega} = \mathbf{\Sigma}_z - \mathbf{H}\left(\mathbf{H}^T\mathbf{W}\mathbf{H}\right)^{-1}\mathbf{H}^T \tag{17}$$

In (17), $\mathbf{\Sigma}_z$ is the covariance of the measurement errors in the input vector $\mathbf{z}$, while $\mathbf{H}$ and $\mathbf{W} = \mathbf{\Sigma}_z^{-1}$ are the Jacobian and weighting matrix used in the considered WLS. A bad datum is detected if normalized residuals larger than a certain threshold (typically between 3 and 5) are found. In this case, the largest of the normalized residuals is suspected to be a bad datum and the WLS is repeated removing it from the input measurements.

Both the first and second step apply a conventional bad data detection and identification process, but the following adjustments are introduced to take into account the peculiarities of the proposed decentralized MASE scheme.

- During the first step, if the voltage measurement at the substation is identified as a bad datum, a flag has to be sent so that, in (2), only the number of feeders n that effectively adopted the substation voltage measurement for the estimation process is considered.
- In the local estimation at the first step, voltage bad data can be correctly identified when at least three voltage measurements are available; if only two voltage measurements are present, a voltage bad datum can be detected but not identified, since the two measurements constitute a critical pair. In this case, the bad datum is always attributed to the substation voltage. When the corrupted measurement is really the one at the substation, the local estimation is correctly performed. If the bad datum actually lies in the other voltage measurement, this will be identified (and removed) during the second step.
- During the voltage bad data process at the second step, if the substation measurement is identified as a bad datum, the substation bus voltage estimates of all feeders where this was used at the first step (e.g., those where it is the only available voltage measurement) are automatically discarded.
- When a corrupted voltage measurement is identified at the second step, a local estimation is repeated on the affected feeder(s) to correct the branch current estimates used for the second step current refinement. For this, all the feeder voltage measurements are replaced by the second step estimation of the substation voltage.
- During the current bad data process at the second step, a bad datum can be detected only if the total power or current at the substation transformer is available. However, only the detection (and not the identification)

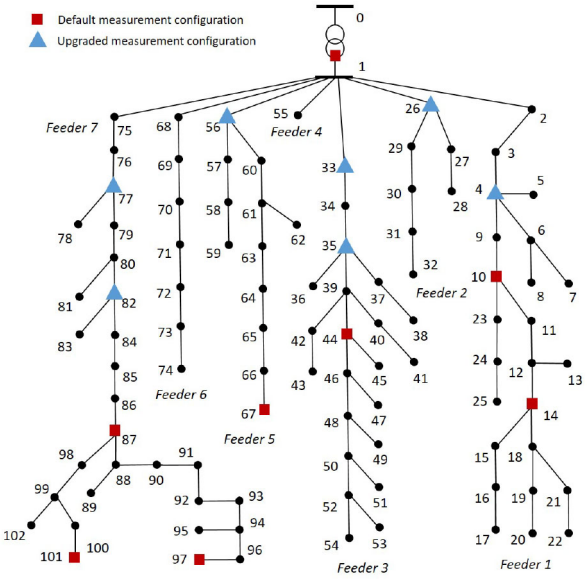

FIGURE 4. Atlantide project distribution grid.

is possible. When a current bad datum is detected, the refinement contributions associated with δI_{i1}^{re} and δI_{i1}^{im} in (12) and (13) are zeroed to avoid spreading the effects of the bad measurement to multiple feeders.

IV. SIMULATION SET-UP

The proposed decentralized MASE for multi-feeder distribution networks has been tested and validated using the grids of the Atlantide project [29]. These grids are Italian distribution networks representative for the rural, urban and industrial scenario. The network depicted in Fig. 4 has been chosen for the simulations presented in this paper, which is a 103-bus grid operated at 20 kV, having 7 long feeders, 5 MV-connected PV plants and about 18 MVA of load at the peak time [23]. Fig. 4 shows the topology of the grid as well as the numbering of the nodes. Branches are numbered considering the largest between the indexes of the nodes they are connected to, decreased by one.

In the tests, the results of the load flow calculation are used as reference values for the operating conditions of the grid. Measurements are extracted by corrupting the reference values with random noise, according to the uncertainty characteristics of the measurement. In particular, an expanded uncertainty equal to 1 % is considered for the real measurements (voltage and power), whereas 50 % is used as expanded uncertainty of the forecast information associated to the pseudo-measurements. A Gaussian distribution is assumed for the associated probability density function and a coverage factor equal to three is used to derive the corresponding standard deviation. Zero injections are modelled as virtual measurements with very high weight.

Fig. 4 shows the measurement configurations considered for the tests. The default measurement configuration is composed of those meters depicted with a red square. Their placement aims at having a different number of meters depending on the feeder, so that it is possible to analyse the accuracy and robustness performance of the estimator(s) also with respect to the number of available devices. Each of these meters provides the voltage magnitude at the bus and the active and reactive power in all the branches converging to that node. To increase the number of measured powers, meters are typically placed in nodes with multiple converging branches. The measurement point at the substation includes the voltage magnitude at the bus and the total power at the substation. The measurements of power at the departure of each feeder can be available or not, depending on the test case. Pseudo-measurements are considered as available for each load or generation node. Beyond the default measurement configuration, an upgraded measurement configuration with additional meters is also considered (blue triangles in Fig. 4). The goal for this is to show how the accuracy performance varies with an increasing number of measurement points and to validate the considerations with a different measurement scenario.

In the following, test results are discussed mainly referring to the Root Mean Square Error (RMSE) of the voltage and current magnitude estimations calculated over 25000 trials of a Monte Carlo (MC) simulation. The results of the proposed MASE approach are compared to those obtained through a WLS-based DSSE performed on the full grid, which in the following is referred to as ISE. Moreover, the results obtained at the first step of the proposed MASE approach (indicated in the following as Feeder State Estimation, FSE) are also presented to underline the improvements achievable through the conceived second step with respect to the case of distributed state estimation without any harmonization procedure.

V. TESTS AND RESULTS

A. TESTS WITH DIFFERENT MEASUREMENT CONFIGURATIONS

In the first test case (Case A), the default measurement configuration shown in Fig. 4 is considered (red squares), here including the availability of power measurements at the departure of each feeder. A benefit of the proposed MASE approach is to allow a significant refinement of the voltage estimation. Figure 5 shows, as an example, the RMSEs obtained for the voltage magnitude estimation at *feeder 2*. It is possible to observe that, thanks to the conceived second step of the MASE, a significant accuracy improvement can be achieved with respect to the FSE (which does not have any harmonization procedure). Moreover, the proposed MASE obtains accuracy results almost identical to those of the ISE, proving that the designed second step minimizes the degradation of the accuracy performance associated with the distributed approach (in comparison with a centralized procedure). The same considerations done for the voltage magnitude estimation in *feeder 2* also hold for the other feeders of the grid. Table 1 summarizes the results for each feeder, showing the average RMSEs (average among all

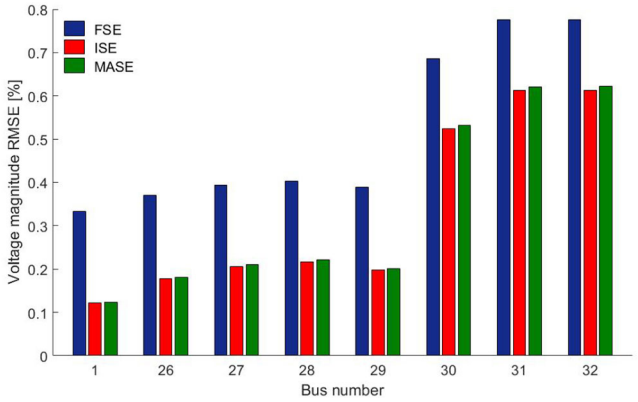

FIGURE 5. Case A, RMSE of the voltage magnitude estimation for feeder 2.

TABLE 1. Case A, average voltage magnitude estimation RMSEs.

Zone	Average RMSE [%]		
	FSE	ISE	MASE
Feeder 1	0.19	0.12	0.12
Feeder 2	0.44	0.27	0.27
Feeder 3	0.26	0.22	0.22
Feeder 4	0.33	0.12	0.12
Feeder 5	0.24	0.12	0.12
Feeder 6	0.34	0.12	0.12
Feeder 7	0.17	0.13	0.13

the nodes of the feeder). In the FSE, the obtained accuracies strictly depend on the number of meters available in the feeder. Thanks to the second-step, the MASE clearly improves the FSE results and MASE RMSEs are equal to those given by the ISE. This confirms the capability of the proposed approach to decouple the DSSE among the feeders of the grid, while achieving voltage estimation accuracies almost identical to the centralized solution.

Regarding the current estimation, the effects brought by the partition of the DSSE problem in multiple areas are more local than the voltage and concentrated at the boundary zones of the sub-areas. For this reason, the maximum effects can be observed at the first branch of each feeder. However, when power measurements are available in those branches, the difference among centralized and distributed solutions is minimal, since the current magnitude estimation mainly depends on the measurement locally available [30]. The RMSE for the current magnitude at the head of the feeders is always around 0.3 % for the ISE, while FSE and MASE have slightly worse results with an RMSE that can reach 0.4 % for some feeders. In general, the MASE always provides better current magnitude estimations than the FSE, but the differences are not so relevant (note that, in general, the uncertainties on current and power estimations are significantly larger than these levels, as it will be also shown in the next sections).

TABLE 2. Case B, average voltage magnitude estimation RMSEs.

Zone	Average RMSE [%]		
	FSE	ISE	MASE
Feeder 1	0.17	0.09	0.09
Feeder 2	0.25	0.09	0.09
Feeder 3	0.17	0.08	0.08
Feeder 4	0.33	0.08	0.08
Feeder 5	0.20	0.09	0.09
Feeder 6	0.34	0.09	0.09
Feeder 7	0.14	0.09	0.09

To confirm the above considerations and results, further tests have been carried out considering an upgraded measurement configuration with additional meters (blue triangles in Fig. 4, Case B). Table 2 shows the average RMSE of the voltage magnitude estimation at each feeder, which can be compared with the results in Table 1. It is possible to notice that only the feeders with additional meters exhibit a lower RMSE for the FSE. In a similar way, ISE provides better estimation accuracies as a consequence of the larger number of available measurements. Also in this scenario, MASE confirms its capability to improve FSE results and to provide accuracy performance almost equivalent to those of the ISE. Similarly to Case A, the RMSE for the current estimates is around 0.2 % or 0.3 % for the first branch of each feeder when considering the ISE, while it is slightly worse (up to 0.4 %) for FSE and MASE (with MASE providing only relatively small improvements with respect to FSE).

B. TESTS WITH UNCERTAINTY IN THE LINE PARAMETERS

Together with the scarce coverage of meters, another main challenge for the monitoring of distribution grids is the accurate knowledge of the grid models. Line parameters are often roughly known or modelled at distribution level, thus bringing additional uncertainties that may affect the estimators' performance [31]. Given this scenario, it is important to analyse the performance of the proposed MASE also in presence of uncertainty in the line parameters and to assess if this source of uncertainty could lead to a more pronounced degradation of the results with respect to the ISE. To this purpose, tests have been performed (Case C) considering the default measurement configuration and line parameters affected by random errors within ± 20 % (with uniform distribution) of the actual value (a quite high uncertainty is chosen to stress the estimators for the purposes of the analysis).

Figure 6 shows the results obtained at feeder level for the average RMSE of the voltage magnitude estimation in comparison with Case A, where line parameters were assumed to be perfectly known. It is possible to observe that the uncertainty in the line parameters is responsible for a degradation of the accuracy performance. This degradation is more

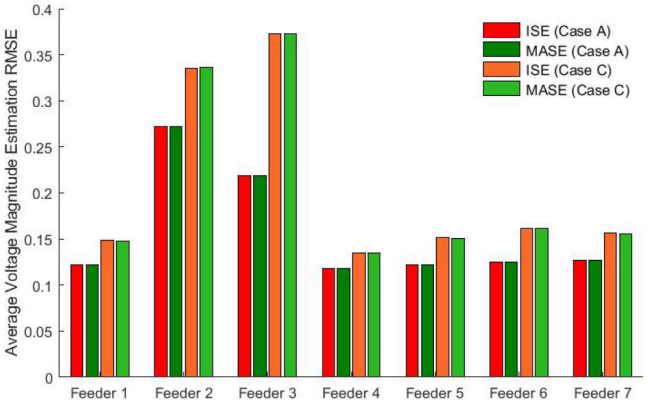

FIGURE 6. Average voltage magnitude estimation RMSEs in presence of line parameter uncertainties.

relevant in those feeders where high power flows, and consequently high voltage drops, are present (namely, feeders 2 and 3). At the same time, however, the simulation results prove that MASE is not more sensitive than ISE to this particular source of uncertainty. This is confirmed by the fact that, also in presence of line parameter uncertainty, MASE is still able to reach estimation accuracies equivalent to those of ISE. Similar considerations hold also when looking at the current estimates. When considering the grid model uncertainty, a degradation of the performance is found for all the estimators, but the performance of MASE in comparison to ISE and FSE follows the same trend already described for Cases A and B.

C. TESTS WITH MISSING MEASUREMENTS AT THE FEEDERS' HEAD

Previous results apparently suggest that the second step to refine the current estimation is not so important in a scenario with full observability of the feeders' departure. However, bad data or measurement losses could occur in some cases, due to malfunctioning of a device or its temporary unavailability. Table 3 shows the current magnitude RMSEs for the first branch of each feeder when its power measurement gets lost, considering the power measurements on all the other feeders' departures as available (Case D, derived from the default measurement configuration). In such a scenario, the proposed second step current refinement leads to a significant estimation improvement. In feeder 2, for example, if the power measurement on branch 25 is lost, its current magnitude RMSE would decrease from about 23 % to 2 % using the proposed MASE. In general, significant benefits can be found for all the feeders, and the proposed second step allows getting results again very close to those of the ISE.

Another possible scenario is given by the presence of the power measurement only at the secondary of the substation transformer and the unavailability of measurements at the start of each feeder (Case E). Fig. 7 shows the RMSE results for the current magnitude estimation of the first branch of

TABLE 3. Case D, current magnitude RMSEs on the first branch of a feeder with a lost measurement.

Feeder with lost measurement	Current magnitude RMSE [%]		
	FSE	ISE	MASE
Feeder 1	3.92	1.08	1.17
Feeder 2	23.35	2.27	2.36
Feeder 3	8.20	0.49	3.95
Feeder 4	13.58	8.60	8.94
Feeder 5	3.65	1.03	1.14
Feeder 6	5.95	0.65	0.68
Feeder 7	2.24	1.00	1.08

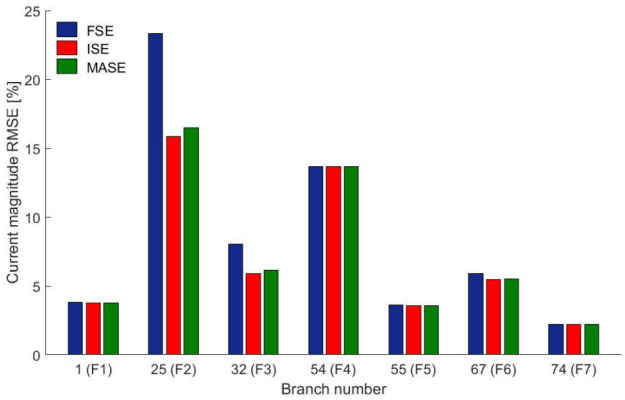

FIGURE 7. Case E, RMSE of the current magnitude estimation for the departing branch of each feeder.

each feeder for this test case. It is possible to notice that, for some of the feeders, the FSE results are already comparable to the ISE results. However, for some other branches (e.g., branches 25 and 32), a significant difference in the accuracy performance exists. In these cases, the integration of the power measurement at the substation made in the second step of the MASE procedure allows enhancing the FSE results and leads to accuracy performance very close to the ISE solution.

D. TESTS WITH BAD DATA

A final set of simulations has been run to assess the robustness of the proposed MASE to bad data, using the default measurement configuration with all the power measurements both at the substation and at the departures of the feeders. The first series of tests considers the case of single bad datum (Case F). For the case of voltage bad data, the corrupted voltage magnitude measurements have been assumed to have a (small) offset of 3 %. Tests showed that, as expected, if the bad voltage is on a feeder with more than two measurements, the bad datum can be correctly identified already during the first step estimation. This always leads to an unbiased estimation and to accuracy performance very close for the ISE and the MASE, similar to what shown in Tables 1 and 3

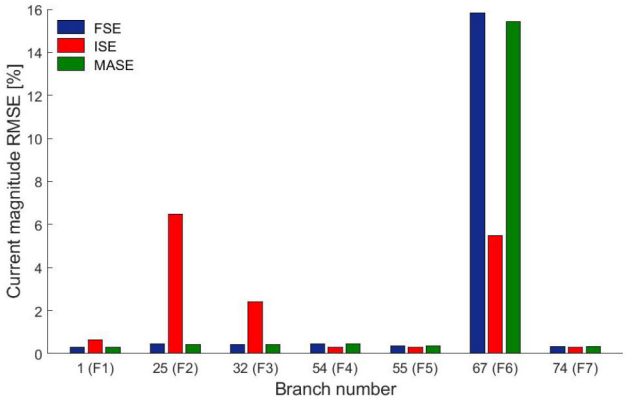

FIGURE 8. Case F, RMSE of the current magnitude estimation for the departing branch of each feeder in presence of bad power input at branch 67.

and in Fig. 5 and 7. If the bad voltage is instead on a feeder with only two voltage measurements, the MASE is usually able to detect an erroneous voltage in the first step and then to correctly identify the affected feeder during the voltage refinement procedure at the second step. Only in few cases, when having the bad voltage at bus 44, the first step estimation at feeder 3 mistakenly identifies the power measurement at the feeder head as bad and, during the second step, a wrong identification of the feeder with the erroneous voltage estimation may occur. In the performed tests, however, 93 % of the cases had the correct identification of the bad voltage at bus 44, and this rate would increase with larger bad data (e.g., 99.5 % for a 5 % offset). Finally, with a bad voltage at the substation, the MASE procedure always allowed to correctly identify this voltage measurement as corrupted during the second step.

The bad data in power measurements is more difficult to handle, as the local impact of powers and the presence of inaccurate pseudo-measurements significantly affects the detectability of erroneous power inputs. For these tests, the corrupted power measurements are considered to have a 20 % offset. Fig. 8 shows the exemplary results of current magnitude RMSE at the heads of the feeders when having the bad datum on the power measurement at branch 67 (feeder 6). The figure highlights the different impact that the bad power has on ISE and MASE. In the ISE, the correct identification of the erroneous power was achieved in 88.9 % of the cases (in the other cases, the total power at the substation is mistakenly identified as bad). When the bad data identification is not correct, the wrong power affects the close branches, here including the departing branches of the other feeders. This explains the increase of RMSE, with respect to the FSE, for branches 1, 25 and 32 (at feeders 1, 2 and 3, respectively). In the MASE, instead, the presence of the bad power is either identified during the first step estimation at feeder 6 (12.6 % of the cases) or detected during the current refinement procedure at the second step (87.4 % of the cases). When the bad datum is detected at the second step, the current refinement contributions given by (12) or (13) (depending on whether the bad data is detected on the real or imaginary current) are zeroed and therefore the branch currents remain similar to the first step estimates. As a consequence, the MASE exhibits a relatively high RMSE on the feeder having the bad power (similar to the FSE), but at the same time it avoids propagating the effects of the bad datum towards the other feeders. This solution can be thus beneficial to bound the impact of the bad power only within the really involved feeder.

Similar considerations hold also for the case of multiple bad data. In this scenario, it is possible to differentiate the cases where bad data belong to the same feeder or to different ones. In the case of bad voltage measurements within the same feeder, when the bad data cannot be removed already in the first step, they are usually detected and identified in the following step. Tests performed applying a 3 % offset in voltage measurements at feeder 1 (nodes 10 and 14) and feeder 7 (nodes 87 and 101) show that a correct identification of the erroneous feeder at the second step is successfully achieved in 100 % and 96.8 % of the cases, respectively. When the bad data are on different feeders and are not already removed at the first step, the second step still allows finding all the feeders with a bad voltage estimate, iteratively. Tests with a 3 % offset for the voltage measurements at nodes 44 (feeder 3) and 67 (feeder 5) gave a correct identification of both the corrupted feeders in 91.2 % of the cases. This percentage increases up to 99.6 % if larger errors in the bad data (5 % offset) are considered. For the sake of comparison, in all the above tests, the ISE provides a correct bad data detection and identification in more than 99 % of the cases.

For the case of bad data in the power measurements, in the proposed MASE, as already discussed, if the bad data are not correctly identified in the first step, only their detection is then possible during the second step. The only difference here is the possibility to have multiple feeders simultaneously affected by the bad data. Coherently with what shown in Fig. 8, in this case, the degradation of the current estimation will be extended to all the feeders affected by a corrupted power. Tests performed with a 20 % offset for the power measurements at branches 1 (feeder 1) and 66 (feeder 6) confirm that the MASE can detect the presence of bad data in the power measurements in all those cases where at least a corrupted current estimate is forwarded to the second step. In this scenario, the ISE provides the correct identification of both the bad data in only 3.4 % of the cases (at least one of them in 59.7 % of the cases), thus highlighting how the identification of bad power measurements is in any case challenging also for centralized DSSE solutions.

E. COMPUTATION TIMES

Overall, the presented results show that the proposed MASE design is able to bring the benefits associated with the distribution of the DSSE (see Sections II and III) while keeping accuracy performance very close to those given by the ISE, for both voltage and current estimations. Furthermore, one of the main advantages given by the proposed multi-feeder

TABLE 4. Average computation time, case A.

	ISE	MASE		
		1st step	2nd step	Total
Avg time [ms]	14.67	1.97	0.37	2.33

partition is the possibility to parallelize the DSSE execution on the different feeders. Table 4 compares the average computation times for the algorithms obtained for Case A during the MC simulation for both the centralized (ISE) and decentralized (MASE) approaches (tests are run in MATLAB 2016 using a PC with a 3.3-GHz CPU and 8 GB of RAM). The computation time for the MASE is calculated by considering the largest execution time for each feeder at both the first and second step, since these would be the bottlenecks for the achievement of the final results.

With the proposed distributed approach, the overall execution time is reduced of more than 80 % (almost an order of magnitude). This confirms the potential of the proposed method to combine the needs of computation speed and accuracy for the DSSE of large distribution grids. In fact, while with the considered grid the execution times are quite low also for the ISE, these would significantly increase for larger grids with thousands of nodes, thus emphasizing the benefits associated with DSSE parallelization. Moreover, some distribution scenarios require to adopt three-phase grid models, thus bringing a further increase of the system size and of the computational burden. Finally, the proposed WLS-based procedure requires repeating from scratch the WLS process when bad data are found. For the ISE, this implies repeating the WLS on the entire grid for each of the discovered bad data. For the MASE, if bad data are found during the first step, this would lead to repeating the first step only for the affected feeder. In case of multiple bad data, if these are on different feeders, the MASE would thus allow parallelizing also the repetition of the first step WLS, leading in this way to an even more important reduction of the overall execution times (with respect to ISE).

VI. CONCLUSION

This paper presented the design of a MASE solution tailored to multi-feeder distribution grids. The conceived solution is based on two sequential steps, both executed locally on each feeder, which involve a first local estimation and a second step harmonization to integrate the boundary results coming from the other feeders. The proposed MASE approach thus allows decoupling the state estimation problem on the different feeders guaranteeing, among others, the distribution of computational burden, communication requirements and storage resources. Moreover, the specific design of the harmonization procedure at the second step allows minimizing the degradation of the accuracy performance with respect to the benchmark results given by the ISE (state estimation on the full grid), for both voltage and current estimations, while guaranteeing similar robustness performance with respect to bad data. As a consequence, the designed distributed estimator can be conveniently used in large multi-feeder distribution grids to divide the state estimation problem while ensuring as accurate as possible results, in line with those achievable by a state estimator applied to the overall grid.

REFERENCES

[1] J. Fan and S. Borlase, "The evolution of distribution," *IEEE Power Energy Mag.*, vol. 7, no. 2, pp. 63–68, Mar./Apr. 2009.

[2] G. T. Heydt, "The next generation of power distribution systems," *IEEE Trans. Smart Grid*, vol. 1, no. 3, pp. 225–235, Dec. 2010.

[3] A. P. S. Meliopoulos, E. Polymeneas, Z. Tan, R. Huang, and D. Zhao, "Advanced distribution management system," *IEEE Trans. Smart Grid*, vol. 4, no. 4, pp. 2109–2117, Dec. 2013.

[4] G. N. Korres, "A distributed multiarea state estimation," *IEEE Trans. Power Syst.*, vol. 26, no. 1, pp. 73–84, Feb. 2011.

[5] A. Conejo, S. De La Torre, and M. Canas, "An optimization approach to multiarea state estimation," *IEEE Trans. Power Syst.*, vol. 22, no. 1, pp. 213–221, Feb. 2007.

[6] M. Zhao and A. Abur, "Multi area state estimation using synchronized phasor measurements," *IEEE Trans. Power Syst.*, vol. 20, no. 2, pp. 611–617, May 2005.

[7] V. Kekatos and G. B. Giannakis, "Distributed robust power system state estimation," *IEEE Trans. Power Syst.*, vol. 28, no. 2, pp. 1617–1626, May 2013.

[8] W. Jiang, V. Vittal, and G. T. Heydt, "A distributed state estimator utilizing synchronized phasor measurements," *IEEE Trans. Power Syst.*, vol. 22, no. 2, pp. 563–571, May 2007.

[9] A. Gómez-Expósito, A. de la Villa Jaen, C. Gómez-Quiles, P. Rosseaux, and T. Van Cutsem, "A taxonomy of multi-area state estimation methods," *Electr. Power Syst. Res.*, vol. 81, no. 4, pp. 1060–1069, Apr. 2011.

[10] D. D. Giustina, M. Pau, P. A. Pegoraro, F. Ponci, and S. Sulis, "Electrical distribution system state estimation: Measurement issues and challenges," *IEEE Instrum. Meas. Mag.*, vol. 17, no. 6, pp. 36–42, Dec. 2014.

[11] A. Gomez-Exposito, A. Abur, A. de la Villa Jaen, and C. Gomez-Quiles, "A multilevel state estimation paradigm for smart grids," *Proc. IEEE*, vol. 99, no. 6, pp. 952–976, Jun. 2011.

[12] A. Angioni *et al.*, "Design and implementation of a substation automation unit," *IEEE Trans. Power Del.*, vol. 32, no. 2, pp. 1133–1142, Apr. 2017.

[13] M. Pau *et al.*, "Design and accuracy analysis of multilevel state estimation based on smart metering infrastructure," *IEEE Trans. Instrum. Meas.*, vol. 68, no. 11, pp. 4300–4312, Nov. 2019.

[14] L. D. A. Garcia and S. Grenard, "Scalable distribution state estimation approach for distribution management systems," in *Proc. 2nd IEEE PES Int. Conf. Exhibit. Innov. Smart Grid Technol. (ISGT Europe)*, Dec. 2011, pp. 1–6.

[15] N. Nusrat, M. Irving, and G. Taylor, "Development of distributed state estimation methods to enable smart distribution management systems," in *Proc. Int. Symp. Ind. Electron. (ISIE)*, Jun. 2011, pp. 1691–1696.

[16] N. Nusrat, P. Lopatka, M. R. Irving, G. A. Taylor, S. Salvini, and D. C. H. Wallom, "An overlapping zone-based state estimation method for distribution systems," *IEEE Trans. Smart Grid*, vol. 6, no. 4, pp. 2126–2133, Jul. 2015.

[17] C. Muscas, M. Pau, P. A. Pegoraro, S. Sulis, F. Ponci, and A. Monti, "Multiarea distribution system state estimation," *IEEE Trans. Instrum. Meas.*, vol. 64, no. 5, pp. 1140–1148, May 2015.

[18] M. Pau, F. Ponci, A. Monti, S. Sulis, C. Muscas, and P. A. Pegoraro, "An efficient and accurate solution for distribution system state estimation with multiarea architecture," *IEEE Trans. Instrum. Meas.*, vol. 66, no. 5, pp. 910–919, May 2017.

[19] I. Dzafic, D. Ablakovic, and S. Henselmeyer, "Real-time three-phase state estimation for radial distribution networks," in *Proc. IEEE Power Energy Soc. Gen. Meeting*, 2012, pp. 1–6.

[20] N.-C. Yang and H.-C. Chen, "Three-phase power-flow solutions using decomposed quasi-Newton method for unbalanced radial distribution networks," *IET Gener. Transm. Distrib.*, vol. 11, no. 14, pp. 3594–3600, 2017.

[21] J. C. Lopez, P. P. Vergara, C. Lyra, M. J. Rider, and L. C. P. da Silva, "Optimal operation of radial distribution systems using extended dynamic programming," *IEEE Trans. Power Syst.*, vol. 33, no. 2, pp. 1352–1363, Mar. 2018.
[22] E. Schweitzer, A. Scaglione, A. Monti, and G. A. Pagani, "Automated generation algorithm for synthetic medium voltage radial distribution systems," *IEEE J. Emerg. Sel. Topics Circuits Syst.*, vol. 7, no. 2, pp. 271–284, Jun. 2017.
[23] G. Celli, F. Pilo, G. Pisano, and G. G. Soma, "Reference scenarios for active distribution system according to ATLANTIDE project planning models," in *Proc. IEEE Int. Energy Conf. (ENERGYCON)*, May 2014, pp. 1190–1196.
[24] S. Lu, S. Repo, D. D. Giustina, F. A.-C. Figuerola, A. Löf, and M. Pikkarainen, "Real-time low voltage network monitoring—ICT architecture and field test experience," *IEEE Trans. Smart Grid*, vol. 6, no. 4, pp. 2002–2012, Jul. 2015.
[25] C. Mateo *et al.*, "European representative electricity distribution networks," *Int. J. Elect. Power Energy Syst.*, vol. 99, pp. 273–280, Jul. 2018.
[26] S. Meinecke *et al.*, "SimBench—A benchmark dataset of electric power systems to compare innovative solutions based on power flow analysis," *Energies*, vol. 13, no. 12, p. 3290, 2020.
[27] M. Pau, P. A. Pegoraro, and S. Sulis, "Efficient branch-current-based distribution system state estimation including synchronized measurements," *IEEE Trans. Instrum. Meas.*, vol. 62, no. 9, pp. 2419–2429, Sep. 2013.
[28] A. Abur and A. Gomez-Exposito, *Power System State Estimation: Theory and Implementation*, vol. 24. Boca Raton, FL, USA: CRC Press, Jan. 2004.
[29] F. Pilo *et al.*, "ATLANTIDE—Digital archive of the Italian electric distribution reference networks," in *Proc. CIRED Workshop Integr. Renew. Distrib. Grid*, May 2012, pp. 1–4.
[30] M. Pau, P. A. Pegoraro, A. Monti, C. Muscas, F. Ponci, and S. Sulis, "Impact of current and power measurements on distribution system state estimation uncertainty," *IEEE Trans. Instrum. Meas.*, vol. 68, no. 10, pp. 3992–4002, Oct. 2019.
[31] M. Pau, F. Ponci, A. Monti, P. A. Pegoraro, S. Sulis, and C. Muscas, "An augmented branch current formulation for state estimation in distribution systems," in *Proc. IEEE 11th Int. Workshop Appl. Meas. Power Syst. (AMPS)*, 2021, pp. 1–6.

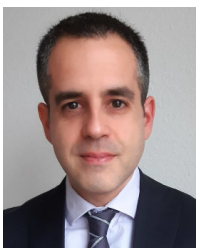

MARCO PAU (Member, IEEE) received the M.S. degree *(cum laude)* in electrical engineering and the Ph.D. degree in electronic and computer engineering from the University of Cagliari, Cagliari, Italy, in 2011 and 2015, respectively. From 2015 to 2021, he was with the Institute for Automation of Complex Power Systems, RWTH Aachen University, Aachen, Germany. Since 2022, he has been a Senior Researcher with the Fraunhofer Institute for Energy Economics and Energy System Technology, Kassel, Germany. His current research interests include the design of solutions for the monitoring and automation of power systems and for the smart management of distribution grids. He is an Associate Editor of the IEEE TRANSACTIONS ON INSTRUMENTATION AND MEASUREMENT.

FERDINANDA PONCI (Senior Member, IEEE) received the Ph.D. degree in electrical engineering from the Politecnico di Milano, Italy, in 2002. She joined the Department of Electrical Engineering with the University of South Carolina, Columbia, SC, USA, as an Assistant Professor, in 2003, and was tenured and promoted in 2008. In 2009, she joined the Institute for Automation of Complex Power Systems with E.ON Research Center, RWTH Aachen University, Aachen, Germany, where she is currently a Professor for Monitoring and Distributed Control for Power Systems. Her research interests include advanced measurement, monitoring and automation of active distribution systems. She is an Elected Member of the Administration Committee of the IEEE Instrumentation and Measurement Society and the Liaison with IEEE Women in Engineering.

ANTONELLO MONTI (Senior Member, IEEE) received the M.Sc. degree *(summa cum laude)* and the Ph.D. degree in electrical engineering from the Politecnico di Milano, Italy, in 1989 and 1994 respectively. He started his career with Ansaldo Industria and then moved in 1995 to Politecnico di Milano as an Assistant Professor. In 2000, he joined the Department of Electrical Engineering with the University of South Carolina as Associate and then a Full Professor. Since 2008, he has been the Director of the Institute for Automation of Complex Power System within the E.ON Energy Research Center, RWTH Aachen University. Since 2019, he holds a double appointment with Fraunhofer FIT where he is developing the new Center for Digital Energy, Aachen. He is the author or co-author of more than 400 peer-reviewed papers published in international journals and in the proceedings of international conferences. He was a recipient of the 2017 IEEE Innovation in Societal Infrastructure Award. He is an Associate Editor of the IEEE SYSTEM JOURNAL, *IEEE Electrification Magazine*, and a Member of the editorial board of the *Sustainable Energy, Grids and Networks* (Elsevier) and the founding board of the *Energy Informatics* (Springer).

CARLO MUSCAS (Senior Member, IEEE) received the M.S. degree *(cum laude)* in electrical engineering from the University of Cagliari, Cagliari, Italy, in 1994. He was an Assistant Professor and an Associate Professor with the University of Cagliari from 1996 to 2001 and from 2001 to 2017, respectively, where he has been a Full Professor of Electrical and Electronic Measurement since 2017. He has authored and coauthored more than 180 scientific articles. His current research interests include the measurement of synchronized phasors, the implementation of distributed measurement systems for a modern electric grid, and the study of power quality phenomena. He is currently the Chairman of the TC 39 Measurements in Power Systems of the IEEE Instrumentation and Measurement Society.

PAOLO ATTILIO PEGORARO (Senior Member, IEEE) received the M.S. degree *(summa cum laude)* in telecommunication engineering and the Ph.D. degree in electronic and telecommunication engineering from the University of Padua, Padua, Italy, in 2001 and 2005, respectively. From 2015 to 2018, he was an Assistant Professor with the Department of Electrical and Electronic Engineering, University of Cagliari, Cagliari, Italy, where he is currently an Associate Professor. He has authored or coauthored over 120 scientific papers. His current research interests include the development of new measurement techniques for modern power networks, with attention to synchronized measurements and state estimation. He is a member of TC 39 (Measurements in Power Systems) and of IEC TC 38/WG 47. He is an Associate Editor of the IEEE TRANSACTIONS ON INSTRUMENTATION AND MEASUREMENT.